Dynamics of Ion Exchange in Partially Sulfonated Polystyrene Ionomer Solutions As Monitored by Stopped-Flow Fluorescence Measurements

Kenneth C. Dowling and J. K. Thomas*

Department of Chemistry & Biochemistry, University of Notre Dame, Notre Dame, Indiana 46556

Received January 25, 1991; Revised Manuscript Received February 7, 1991

ABSTRACT: Stopped-flow studies were used to investigate the transport of ionic materials in ionomers. The exchange of ionic materials in PS-1.7 ionomer solutions was approximated by a two-component, time-dependent diffusion model. This model is developed based on the shell–core structural model suggested by our prior work. The time-independent components were shown to be limited by the rates of ionomer and, hence, ion aggregate reorientations. The diffusion-limited, time-dependent components were interpreted as a consequence of the slow ion migration through the mantle of the aggregates. The invariance of exchange kinetics as ionomer concentrations were increased provides evidence to support the proposal that ion aggregates retain their intramolecular nature even at high concentrations where intermolecular forces dominate the rheological characteristics. The dynamics of polymer conformational adjustment was observed to be rapid upon the addition of a polar solvent, which acts to reduce binding forces in the ion aggregates. This rapid readjustment suggests a highly strained polymer backbone configuration in the aggregated state.

Introduction

The kinetics of ion and ion pair exchange of ionomers in solution and their implications to ionic reactions in hydrophobic media are important, particularly to the field of polymer chemistry. In anionic polymerizations, a bimodal molecular weight distribution arises when ion pair interchange is slow.[1,2] It has also been proposed that the rheology of ionomers, both in bulk and in solution, should be sensitive to the rates of ion pair interchange.[3,4] However, only recently have studies of the dynamics of ionic interchange in ionomer solutions been reported.[5,6] This study by Morawetz and Wang[5] provides background for the present study. They studied the exchange of large organic ions via long-range energy transfer in dioxane solutions of partially sulfonated polystyrene ionomers. Our study monitors short-range ion exchange of Cu^{2+} in toluene solutions of these ionomers. There are some differences in the behavior of the system studied in this paper and that in ref 5. Here, the use of divalent cations and of toluene as a solvent makes for more stable ion clusters than that in ref 5. Also quenching requires closer contact than energy transfer between the interacting ions. The present work used the sodium salt of the sulfonated PS as the starting material, while ref 5 used the sulfonated PS in the acid form. Such investigations encounter considerable difficulty in interpretation of results due to the complexity of polymer systems.

Polymer systems, in general, are complex due to their polydispersity. A distribution of molecular weights, for example, leads to variations in the properties and characteristics on a molecular scale. The partially sulfonated polystyrene ionomers, in addition, have a random placement of the ionic units on the polymer chains.[7] The relative positions of ionic groups affects ion aggregation size, mobility, and binding strength, among other properties. Studies of ionomer solutions at equilibrium provide an estimate of the average conditions of the systems. The preceding paper[8] demonstrates, for example, that salt added to ionomer solutions in toluene are incorporated into the ionic clusters of the ionomer. A dynamic investigation, however, can help elucidate the effects of the distribution of ion aggregate properties.

Dynamic measurements allow the study of interactions between different species. In the case of ionomers, the results can be interpreted in terms of mechanisms of ion exchange and, thereby, elucidate the properties of these amphiphilic systems. A standard analytical technique for measuring the dynamics of reaction is the stopped-flow technique. In conjunction with a spectrofluorimeter, the change in fluorescence intensity upon rapid mixing in the stopped-flow cell of two reactants can report on the rate of reaction. This paper presents the results of a dynamic, stopped-flow investigation of ion exchange in solutions of a 1.7% sulfonated polystyrene ionomer (PS-1.7).

In the dynamic investigations that follow, two ionomer solutions containing different ionic species are mixed, and the emission intensity of a fluorescent probe is monitored as the mixed system comes to a final equilibrium state. For example, a solution of ionomer doped with the fluorescent probe, $Ru(bpy)_3^{2+}$, is mixed with one doped with Cu^{2+}, a fluorescence quencher. Initially, the probe is located in ion aggregates that are free of quencher and exhibit their normal fluorescence. As ions exchange, quencher and probe may occupy the same sites and the overall fluorescence intensity decreases. At final equilibrium, a constant fluorescence intensity is achieved, which is proportional to the number of vacant sites of the quencher; the quenching is static in nature and is proportional to the ratio of copper ion to ionic aggregates, as determined in the previous study.[8] Measuring the change in fluorescence intensity as a function of time provides a means of analyzing the kinetics of ion exchange in ionomer solutions. The effects of polymer concentration, inert salts, probes, and quencher loadings on the kinetics of ion exchange in PS-1.7 solutions in toluene were investigated. Also, the rates of disruption of ionic aggregates upon addition of a polar solvent were examined.

Experimental Section

Materials. The toluene used was HPLC grade obtained from Aldrich and used without further purification. Spectrophotometric grade anhydrous methanol was used as received from Mallinckrodt. Partially sulfonated polystyrene (PS-1.7) was

* Author to whom correspondence should be addressed.

0024-9297/91/2224-4131$02.50/0

generously provided by Dr. R. D. Lundberg, Exxon Chemicals Co. [4-(1-Pyrenyl)butyl]trimethylammonium bromide. (PN^+) was used as received from Molecular Probes, Inc. Tris(2,2'-bipyridyl)ruthenium(II) chloride hexahydrate (Ru(bpy)) was used as received from Aldrich. Other materials were reagent grade or better and used as received.

Polymers and Preparations. The 1.7 mol % sulfonated polystyrene ionomer solutions were prepared as described previously.[8]

Instrumentation. Steady-state fluorescence measurements wre predominantly made on an SLM/Aminco SPF-500C spectrofluorimeter. This instrument utilizes a xenon arc lamp operating at 250 W as an excitation source. A Hamamatsu R928P photomultiplier tube (PMT) is included as detector. Data were transferred to a Zenith PC microcomputer for storage and analysis.

A customized adaptation of the Tri-tech Dynamic Instruments Model IIA apparatus was utilized in conjunction with the SLM/Aminco SPF-500C spectrofluorimeter for stopped-flow experiments. The two solutions to be mixed are introduced into the two 2.5-mL syringes, which are driven by a pneumatic piston driven at 20 psig; flow is initiated by opening the pneumatic valve. The solutions are mixed in a 12 × 2 × 2 mm quartz cell with 3-ms dead time, where the fluorescence is monitored by the SLM/Aminco fluorimeter. The effluent syringe simultaneously halts the flow and triggers the data acquisition by closing electrical contact across the external trigger port of the SPF-500C fluorimeter. In addition to the characteristics described previously, the fluorimeter operating in the "Kinetics" mode provides the capability to store up to 500 data points separated by as few as 1 ms/point. The rise time of the SPF-500C was measured to be 5 ms, resulting in a total response time of the stopped-flow experiments of about 8 ms.

All of the stopped-flow experiments were conducted at 19 °C. In each experiment, the two syringes were loaded with the different ionomer solutions to be mixed. The pneumatic drive injected equal volumes of the solutions through the cell. The effluent syringe simultaneously stopped flow through the cell and closed the electrical contact, which triggered the measurement of the "steady-state" fluorescence intensity of the mixture in the cell as a function of time. The results were interpreted in terms of the proximity of quenchers and probes, yielding information used to evaluate the dynamics of ion exchange in the ionomer systems.

Results and Discussion

Exchange of Cu^{2+}. Ionomer solutions, 5 g/L PS-1.7 in toluene, were prepared with varying Cu^{2+} loadings in order to gauge the quencher's effects on the exchange kinetics. Ca^{2+} was added in appropriate concentrations to maintain constant salt concentration throughout the series of different Cu^{2+} quencher concentrations. Ca^{2+} was selected for its similar charge and size to the quencher and its inertness with regard to $Ru(bpy)_3^{2+}$ quenching. These solutions were mixed in the stopped-flow apparatus with solutions containing the same concentration of ionomer and the same total M^{2+} loading (using only Ca^{2+}) but doped with a small amount of the fluorescent probe, $Ru(bpy)_3^{2+}$.

Low Ionic Loadings. Figure 1 shows the decrease in intensity of emission of the mixed solutions at a total bivalent salt concentration of 0.36 mM. Differences in the individual curves are due to the varying Cu^{2+} concentrations in the series of solutions mixed with the probed solution.

The relatively low loadings of quencher in Figure 1 do not permit enough Cu^{2+} in the initial solutions to fully occupy the ion aggregates in the final mixture. Consequently, the equilibrium intensities increase as $[Cu^{2+}]$ decreases, resulting in the differing baselines for these curves. These baseline values are identical with those predicted by the static measurements of the previous chapter. The kinetics are complex. Qualitatively, the exchange increases only slightly with increasing $[Cu^{2+}]$. The extent of quenching at equilibrium is decreased proportionally, as predicted from static measurements.

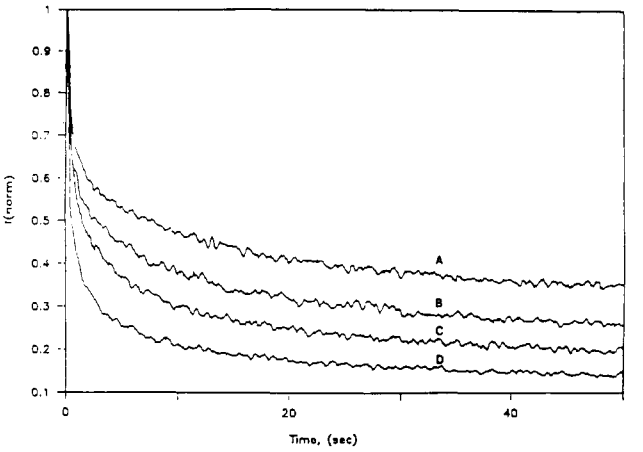

Figure 1. Copper exchange at low ionic loading. All solutions were 5 g/L PS-1.7, 0.36 mM M^{2+}. Solutions mixed with the Ru(bpy) probed ionomer were (A) 0.29 mM Cu^{2+}, (B) 0.31 mM Cu^{2+}, (C) 0.34 mM Cu^{2+}, and (D) 0.36 mM Cu^{2+}. Ca^{2+} was varied to maintain $[M^{2+}]$ = 0.36 mM.

Quantitative considerations require a working model to develop a generalized mechanism from which parameters are analyzed. Chemical changes can then be compared in term of the numerical differences in those kinetic parameters. As discussed earlier, ionomer systems are not expected to fit any simple kinetic schemes. The "shell/core" model,[9] proposed for bulk ionomers, however, provides a starting point for developing a working kinetic scheme.

The proximity of quenchers and probes in the ion aggregate cores was shown in our earlier investigation[8] to be responsible for the unusually efficient quenching. In the stopped-flow experiments, quenching cannot occur unless the Cu^{2+} quencher redistributes among ion aggregates by exchanging to vacant sites; a process requiring diffusion through the aggregate shell. When this diffusion becomes important in the overall rate of reaction, the rate constant must include a time-dependent component analogous to that predicted by the Einstein–Smoluchowski diffusion theory:[10-13]

$$k(t) = k + at^{-1/2} \tag{1}$$

The kinetics can then be written in terms of the emission intensity as a function of time:

$$I(t) = I_0 \exp\{-kt - at^{1/2}\} \tag{2}$$

where "a" describes the transient diffusion behavior and k describes the other processes affecting the rates, including ion aggregate and polymer readjustments.

The stopped-flow intensity decays were fitted to eq 2 after subtracting the baselines and normalizing to maximum intensity. The decays and fits are shown in Figure 2, with the fitted curves at short times provided for each curve in Figure 3. The latter curves cover approximately 80–90% of the intensity change, and therefore the slight deviations at long times are insignificant. The parameters from these fits are provided in Table I, and it is concluded from the negligible values of the time-independent component that the diffusion processes in the polymers are rate-limiting.

Ideally, the diffusion parameter, a, should increase linearly with increasing $[Cu^{2+}]$ as the "driving force" for diffusion is the concentration gradient. However, Figure

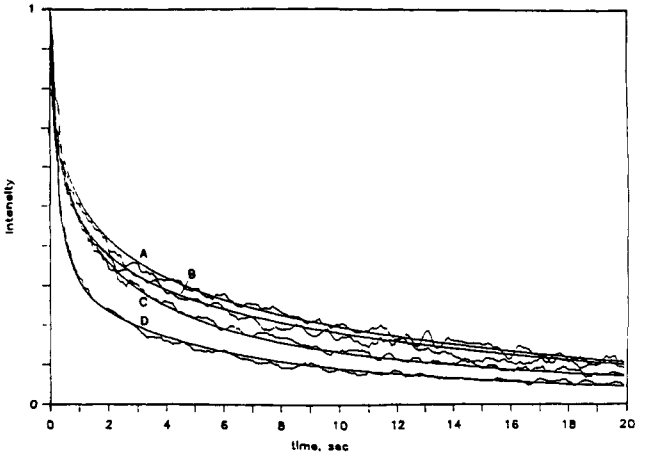

Figure 2. Time-dependent diffusion kinetic fits at low ionic loadings, normalized decays. Solutions mixed with the Ru(bpy) probed ionomer were (A) 0.29 mM Cu^{2+}, (B) 0.31 mM Cu^{2+}, (C) 0.34 mM Cu^{2+}, and (D) 0.36 mM Cu^{2+}. Ca^{2+} was varied to maintain $[M^{2+}] = 0.36$ mM. (See Table I for fitting parameters.)

4 exhibits a moderate deviation from linearity, which is attributed to the chemical changes in the ion aggregates (particularly with respect to varying $[Ca^{2+}]$) intrinsic to the experiments. In the earlier work,[8] the Ca^{2+} concentration was shown to slightly alter the environment for $Ru(bpy)_3^{2+}$ based on a slight blue shift in its emission spectra at high Ca^{2+} loadings. This deviation from linearity is tentatively attributed to the slight change in the chemical nature of the ion aggregates as Ca^{2+} is replaced by Cu^{2+} and vice versa.

High Ionic Loadings. Figure 5 shows the decrease in intensity of emission of the mixed solutions at a total bivalent salt concentration of 0.71 mM along with decay curves fitted to eq 2. The PS-1.7 concentration remained at 5 g/L, and the procedures described above were followed. The resulting parameters are provided in Table II.

In each curve presented in Figure 5, the mixed system contains an excess of quencher. That is, there is enough Cu^{2+} in the initial solutions to fully occupy the sites in the final mixtures, and in each, the emission is totally quenched. There are two components to the kinetics, a time-dependent component and a nonnegligible time-independent component. The nature of the sites is changed by the increased ionic content, based on the qualitative differences between the kinetics in Figures 3 and 5 and corroborated by the transition to include the time-independent component, k. Qualitatively, the initial rapid component is slowed by the higher ionic content, but the slower component is increased in rate.

Both parameters from the time-dependent diffusion model, k and a, increase linearly with $[Cu^{2+}]$ at high M^{2+} loadings, as shown in Figure 6. The diffusion parameter, as stated above, ideally should increase linearly with the quencher concentration gradient and, hence, the Cu^{2+} concentration. The linearity here demonstrates that the chemical nature of the ion aggregates was not so sensitive to the small changes in $[Ca^{2+}]$ as were the ionomer solutions with low ionic loadings. The increase in the time-independent rate is attributed to the necessary experimental changes in $[Ca^{2+}]$. Experimentally, $[Ca^{2+}]$ is decreased as $[Cu^{2+}]$ is increased. Consequently, this parameter *decreases* linearly with increasing $[Ca^{2+}]$. Since the size of the ion aggregates was shown to be essentially constant at constant ionic loading, the time-independent component probably reflects the slowing of the Cu^{2+} exchange as it becomes limited by the transfer between aggregates, or leaving rate, of Ca^{2+}. Although also limited by diffusional process, higher $[Ca^{2+}]$ does not directly affect the observable emission intensity. Also, the ability of ionic material to *leave* an ion aggregate requires prior readjustments in the ionomer and aggregate configurations, which are expected to provide the time-independent component of the kinetics. The effects of Ca^{2+} on the stopped-flow Cu^{2+} exchange kinetics requires further elucidation to confirm these conclusions.

Effects of Total Loading. By varying the concentration of inert Ca^{2+}, the effects of total M^{2+} loading were clarified. At constant PS-1.7 and Cu^{2+} concentrations, the amount of Ca^{2+} in *both* the $Ru(bpy)_3^{2+}$-probe-doped and the Cu^{2+}-doped solutions was varied. Figure 7 presents the resulting fluorescence decays upon mixing with decay curves fitted to eq 2. Ultimately, in each run, the fluorescence was quenched totally. Qualitatively, the initial portion of each curve is slowed by the increasing Ca^{2+} loading. At longer times, the overall rate is increased as the inert salt content is increased. Numerical values are reported in Table III and plotted versus $[Ca^{2+}]$ in Figure 8.

As ion aggregates increase in size to accommodate more external salts, probes in the core may be inhibited from reacting with quenchers at the extremities of those ion aggregates. Thus, the initial exchange is no longer capable of rapidly quenching a probe in any location of the ion aggregate. The necessary counter-exchange of ionic material through a thicker polymer shell slows the measurable rate of decrease in fluorescence intensity, described by the parameter a.

The increase in ion aggregate size accompanies a decrease in binding strength of ions as the ion pair/ion pair attractive forces per sulfonate group are diminished as calculated on the basis of bulk ionomer systems.[14] Ion aggregate readjustments along with configurational changes in the ionomer should be enhanced by the increase in added salts. The time-independent component of the fluorescence decay, described by "k", therefore reflects the intramolecular changes in the ionomer systems and a corresponding increase in this rate with increasing loading is observed. This increase suggests a gradual transition in the properties of the ion aggregates as the Ca^{2+} loading is increased. The magnitude of the values for k are thus affected by changes in the characteristics of the ionic aggregates.

In summary, there is support for the proposed shell/core model for aggregate structure in the dynamic studies of ion exchange in PS-1.7. Exchange of ions between the shells of ion aggregates is relatively fast. Ion migration in the monomers is required to achieve final equilibrium via the internalization of quenchers. The relative importance of the time-dependent and time-independent components of the exchange rate is controlled by the total ionic loading in the ionomer systems. It should be noted that at any loading, a distribution of ion aggregate sizes (and binding strengths) is possible, although it is expected from bulk measurements to be narrow.[15] These results, therefore, are regarded as average effects for these specified conditions.

Probe Effects. Probe Concentration. The effects of probe concentration on the exchange kinetics was measured to eliminate concerns that the two components observed were a result of differing rates of probe and quencher exchange. In Figure 9 the ionomer, Cu^{2+}, and Ca^{2+} concentrations were held constant while the $Ru(bpy)_3^{2+}$ concentration was varied by a factor of 20. No measurable change in the rates, distributions, or equilibrium intensities was evident. Consequently, the effects

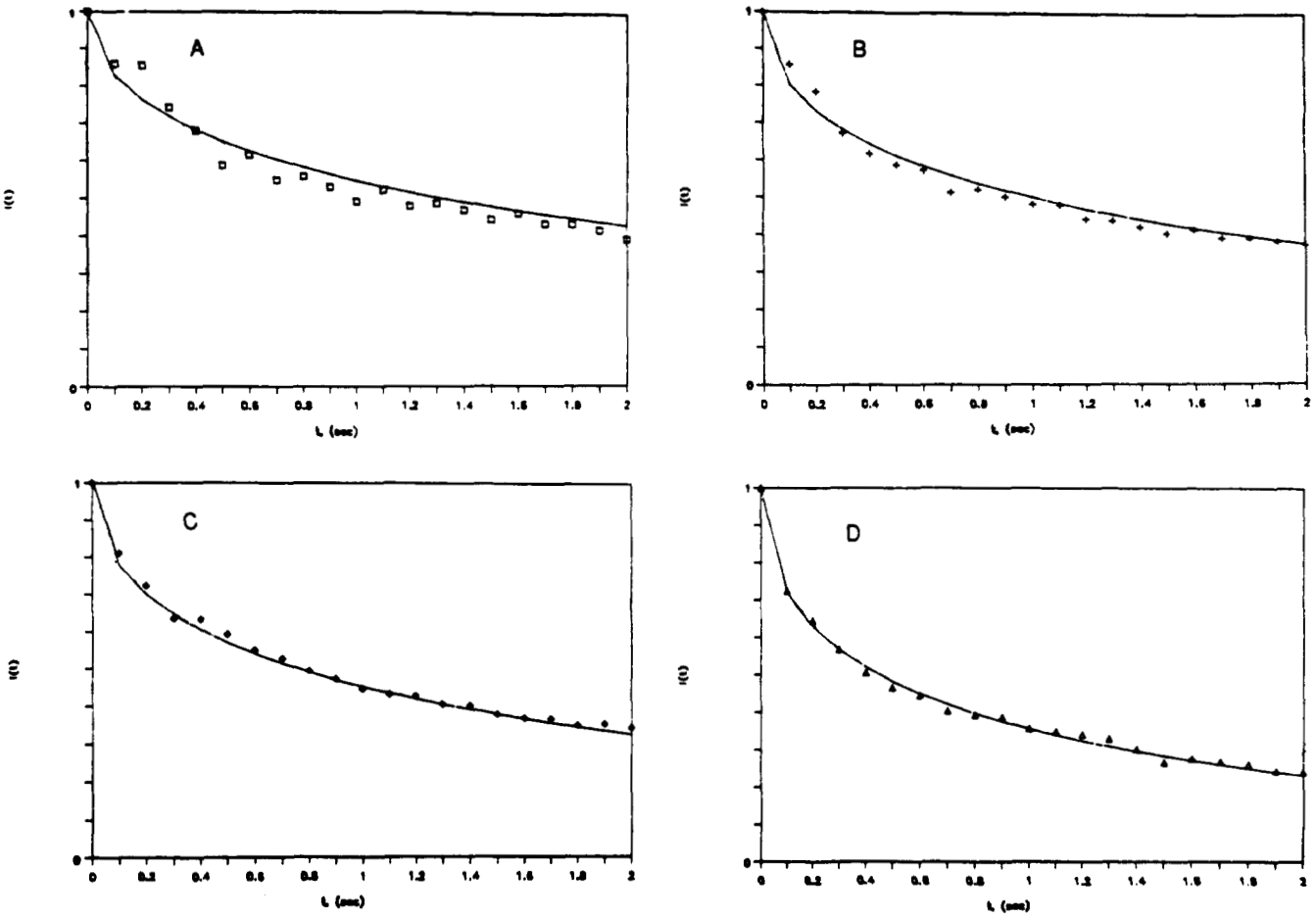

Figure 3. Curve fitting on a fast time scale: Samples labeled as in Figure 2: (A) $k = 4.0 \times 10^{-7}$/s; $a = 0.605/s^{-1/2}$. (B) $k = 1.2 \times 10^{-6}$/s; $a = 0.695/s^{-1/2}$. (C) $k = 1.2 \times 10^{-7}$/s; $a = 0.795/s^{-1/2}$. (D) $k = 1.4 \times 10^{-7}$/s; $a = 1.035/s^{-1/2}$.

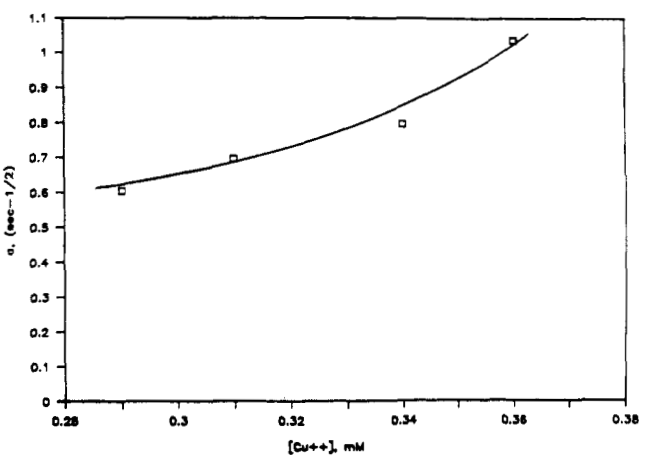

Figure 4. Time-dependent diffusion parameter, a, versus $[Cu^{2+}]$ at low ionic loading (0.36 mM).

Table I
Fitting Parameters for Cu^{2+} Exchange at Low Ionic Loadings (0.36 mM M^{2+})

$[Cu^{2+}]$, mM	k, s^{-1}	a, $s^{-1/2}$	$[Cu^{2+}]$, mM	k, s^{-1}	a, $s^{-1/2}$
0.29	4.0×10^{-7}	0.605	0.34	1.2×10^{-7}	0.795
0.31	1.2×10^{-6}	0.695	0.36	1.4×10^{-7}	1.035

of probe concentration on the sites was negligible, and the exchange kinetics report on the rate of quencher redistribution.

Probe Type. Replacing the $Ru(bpy)_3^{2+}$ probe by PN^+ had no significant effect on the observed kinetics. A sample decay from PN^+ probed systems is provided in Figure 10. Although the most probable location of the emitting head group is extended radially on a four-carbon chain from the ion aggregate core, this had no effect on the observed intensities. This may suggest the shell thickness is large compared to the core radius. However, it eliminates concerns regarding probe effects on the observable kinetics; only changes in the system are observed. That is, the fluorescence probes report on the relative proportion of sites that contain at least one quencher and those that are vacant. Thus, the changes in emission intensity report on the exchange of the ionic quencher between aggregates as

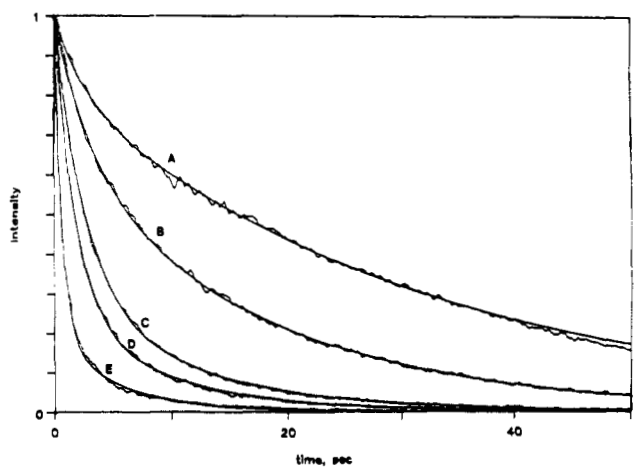

Figure 5. Copper exchange at high ionic loading. All solutions were 5 g/L PS-1.7, 0.72 mM M^{2+}. Solutions mixed with the Ru(bpy) probed ionomer were (A) 0.25 mM Cu^{2+}, (B) 0.33 mM Cu^{2+}, (C) 0.40 mM Cu^{2+}, (D) 0.49 mM Cu^{2+}, and (E) 0.72 mM. Ca^{2+} was varied to maintain $[M^{2+}] = 0.72$ mM. (See Table II for fitting parameters.)

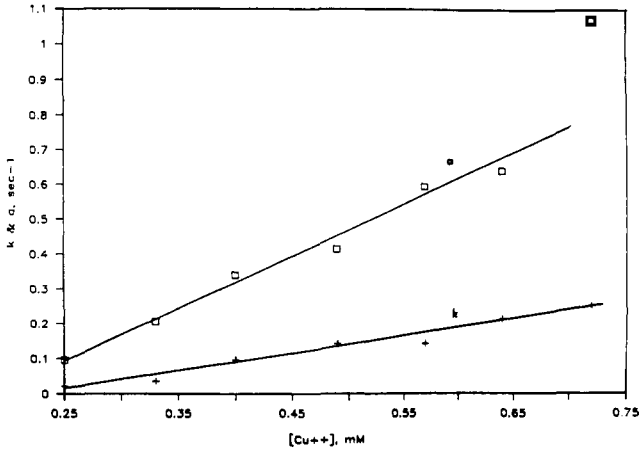

Figure 6. Time-dependent diffusion kinetic parameters versus $[Cu^{2+}]$ at high ionic loading, (0.72 mM).

Table II
Fitting Parameters for Cu^{2+} Exchange at High Ionic Loadings (0.71 mM M^{2+})

$[Cu^{2+}]$, mM	k, s^{-1}	a, $s^{-1/2}$	$[Cu^{2+}]$, mM	k, s^{-1}	a, $s^{-1/2}$
0.25	0.022	0.096	0.57	0.141	0.595
0.33	0.034	0.206	0.64	0.212	0.647
0.40	0.097	0.340	0.72	0.252	1.083
0.49	0.143	0.413			

proposed previously.

Effects of Ionomer Concentration. Variation of the PS-1.7 ionomer concentrations while maintaining a constant ionic loading ($[M^{2+}]$/g of polymer) was conducted. The varying concentrations were prepared by dilution from the 10 g/L solutions. Consequently, Cu^{2+}, $Ru(bpy)_3^{2+}$, and Ca^{2+} concentrations were decreased in proportion to the ionomer concentrations. The resulting stopped-flow decays are presented in Figure 11. Despite the factor of 5 decrease in ion concentrations and a similar decrease in ion aggregate concentrations, the kinetics show that the extent of the slow and fast process varies but that the kinetics are roughly equivalent. This proves the intramolecular processes, migation of ions through the shell, and the readjustments of the ion aggregate core are rate-limiting for any viable exchange mechanism. The two-component mechanism proposed above is supported by these findings.

The small increases in the baseline intensities at the lowest ionomer concentrations can be explained by the results of our earlier studies.[8] Namely, aggregate sizes were found to drop off slightly, below an ionomer concentration of about 5 g/L ionomer. This results in an overall increase in the number of possible sites, decreasing the fraction of which are quenched.

The kinetic parameters in the exchange above 5 g/L remain constant as ionomer concentration is increased. The conclusions from static studies[8] as well as separate investigations[16,17] point to constant coil dimensions as concentration is varied; even when the coils associate. The lack of a change in the kinetics with PS-1.7 concentration, those parameters limited by intra-ion-aggregate phenomena, demonstrates that the integrity of the sites is intact as the ionomer associates at the higher concentrations. The large viscosity of very high ionomer concentrations precludes flow studies under these conditions.

Rates of Aggregate Disruption. Aggregate reorientations, the intramolecular process contributing to the time-independent rate modeled by k in the previous analyses, were isolated experimentally from other processes. Starting with a $Ru(bpy)_3^{2+}$-doped ionomer, which

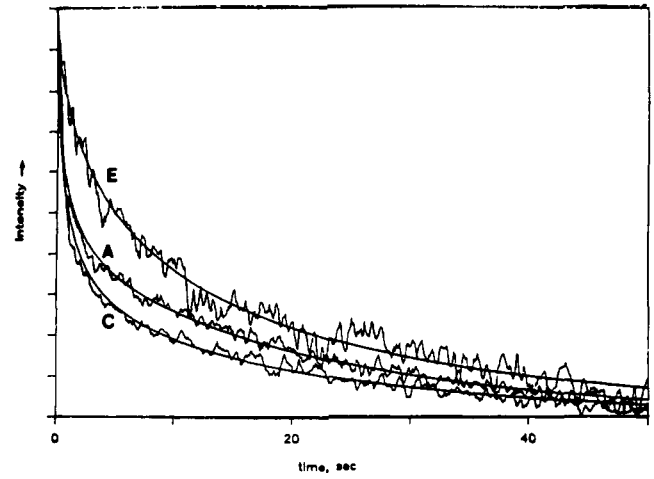

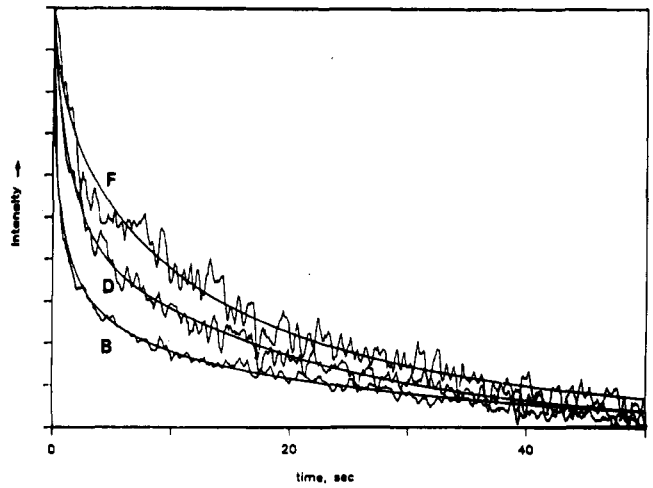

Figure 7. Effect of Ca^{2+} on copper exchange kinetics. All solutions were 5 g/L PS-1.7. Solutions mixed with the Ru(bpy)-probed ionomer were 0.26 mM Cu^{2+} and the following concentrations of Ca^{2+}: (A) 0 mM; (B) 0.09 mM; (C) 0.17 mM; (D) 0.26 mM; (E) 0.35 mM; (F) 0.43 mM. (See Table III for fitting parameters.)

Table III
Fitting Parameters for Cu^{2+} Exchange at Varying Calcium Loadings (0.26 mM Cu^{2+})

$[Ca^{2+}]$, mM	k, s^{-1}	a, $s^{-1/2}$
0.00	1.8×10^{-7}	0.454
0.07	1.4×10^{-7}	0.492
0.17	1.3×10^{-7}	0.503
0.26	0.006	0.384
0.35	0.014	0.276
0.43	0.020	0.241

contained just enough Cu^{2+} to quench all fluorescence, a step change in the number of ion aggregates among which the quenchers could be distributed is accomplished by stopped-flow mixing with an ionomer containing no Cu^{2+}. The emission intensity increases as the ions adjust to their equilibrium distributions. Only half of the sites contain quencher at the final conditions.

According to the proposed mechanisms, ion aggregate reorientation would be required prior to any migrational processes through the shell to affect the expected intensity increases in this experimental setup. Since this is a relatively slow process, the ion aggregate readjustments should be rate-limiting for the overall ion exchange. The increase in intensity is shown to be roughly first order for the ionomer reorientations at this Cu^{2+} loading in Figure 12: $I(t)$ versus time. The exchange rate, $k_{obs} = 0.0352\ s^{-1}$,

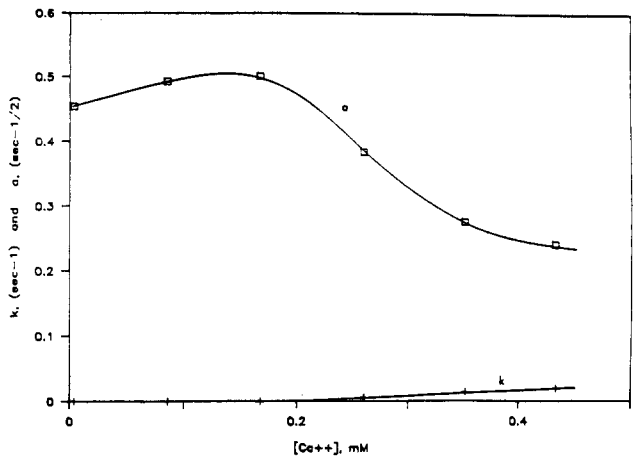

Figure 8. Time-dependent diffusion kinetic parameters versus $[Ca^{2+}]$ at constant Cu^{2+} concentration (0.26 mM).

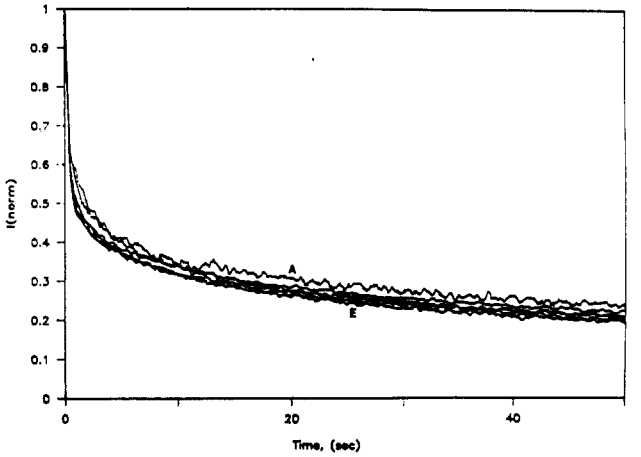

Figure 9. Effects of $Ru(bpy)_3^{2+}$ concentration on observed kinetics. 0.36 mM total M^{2+} loading; 5 g/L PS-1.7. [Ru(bpy)] varies sequentially from (A) 0.005 mM to (E) 0.100 mM.

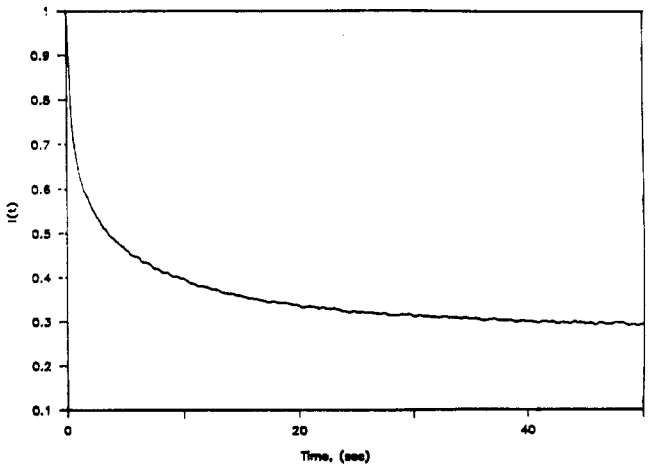

Figure 10. Copper exchange monitored by using the alternate probe, PN^+: 5 g/L PS-1.7; 0.36 mM total M^{2+}; 0.31 mM Cu^{2+}/0.07 mM Ca^{2+} in mixing solution. $k = 2.2 \times 10^{-7}$ /s; $a = 0.674/s^{-1/2}$. Parameters are comparable to those for the Ru(bpy) probed system under identical conditions (re: Table I).

is comparable to those calculated for the slow components of the exchange in Table II, k at 5 g/L PS-1.7 and 0.36 mM total M^{2+} concentrations. This confirms the assignment of ion aggregate reorientation processes to the time-independent component in the time-dependent diffusion kinetic model.

Effects of Methanol Addition. In the presence of as little as 2% v/v anhydrous methanol added to the toluene solvent, the ion exchange reactions become too rapid ($k < 100\ s^{-1}$) to measure by the stopped-flow technique. The rates of polymer readjustment upon the addition of methanol, however, can be measured. A solution of PS-1.7 doped with Ru(bpy) with fluorescence totally quenched by Cu^{2+} was mixed with a similar solution with a varying solvent composition, i.e., varying MeOH concentrations. As ion aggregates open, the quenching efficiency is decreased and emission intensity increases. The rate of ion aggregate breakup is therefore monitored. These results are shown as log plots in Figure 13. The final intensity increases with methanol concentration, as does the rate at which it is approached. These rates are plotted versus [MeOH] in Figure 14. As might be expected, the rate of ion aggregate unraveling increases linearly with the concentration of the polar solvent, methanol.

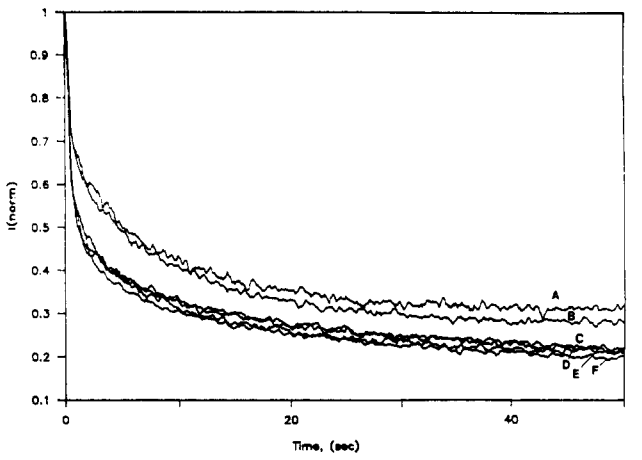

Figure 11. Effects of ionomer concentration on exchange kinetics. Ionomer concentrations vary from (A) 1.76 g/L, (B) 3.52 g/L, (C) 5.28 g/L, (D) 7.04 g/L, (E) 8.80 g/L, to (F) 10.6 g/L; all having the same ratios of ions upon mixing: 35 μM Cu^{2+}/g PS-1.7 and 35 μM Ca^{2+}/g PS-1.7.

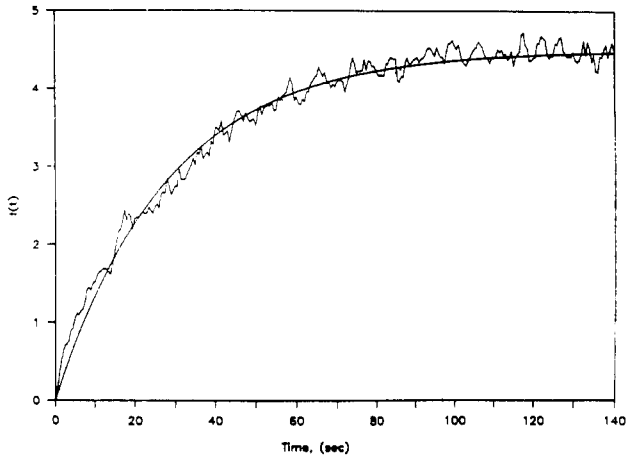

Figure 12. Rate of copper leaving from quenched sites: Ru(bpy)-probed 5 g/L solution of PS-1.7 quenched by 0.24 mM Cu^{2+} was mixed with 5 g/L PS-1.7. Rate of intensity increase is first-order: $k_{obs} = 0.0352/s$.

Conclusions

The exchange of ionic materials in PS-1.7 ionomer solutions was approximated by a two-component, time-dependent diffusion model. This model is developed based on the shell/core structural model suggested by our earlier work.[8] The time-independent components were shown to be limited by the rates of ionomer and, hence, ion aggregate reorientations. The diffusion-limited, time-dependent components were interpreted as a consequence

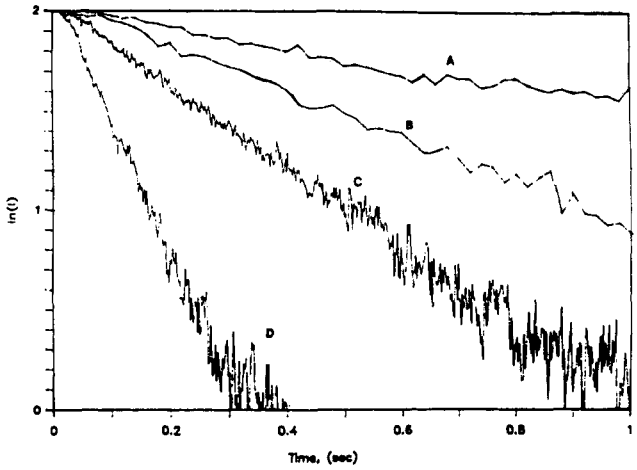

Figure 13. Log plots of the rate of aggregate disruption by methanol. Ru(bpy)-probed 5 g/L PS-1.7, 0.24 mM Cu^{2+}, 0.12 mM Ca^{2+}, mixed with 5 g/L ionomer in solvent consisting of toluene with the following methanol content (% v/v): (A) 2; (B) 5; (C) 10; (D) 30.

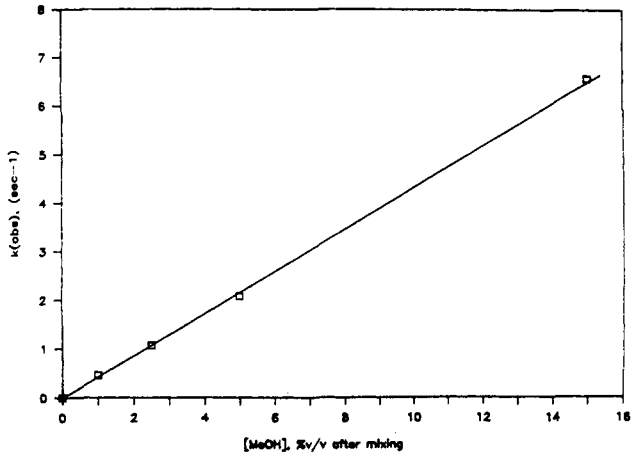

Figure 14. Observed disruption rates versus volume percent methanol in mixed samples.

of the slow ion migration through the mantle of the aggregates. The invariance of exchange kinetics as ionomer concentrations were increased provides evidence to support the proposal[16] that ion aggregates retain their intramolecular nature even at high concentrations where intermolecular forces dominate the rheological characteristics.[17-20] The dynamics of polymer conformational adjustment was observed to be rapid upon the addition of a polar solvent, which acts to reduce binding forces in the ion aggregates. This rapid readjustment suggest a highly strained polymer backbone configuration in the aggregated state.

Acknowledgment. We thank the National Science Foundation, via Grant CHE-89-11-906, for support of this work. Also, funding provided by the Reilly Fellowship at the University of Notre Dame is greatly appreciated. We are especially grateful for the our discussions with and materials provided by Dr. R. D. Lungberg of the Exxon Chemical Co., which made this study possible.

References and Notes

(1) Bhattacharya, D. N.; Lee, C. L.; Smith, J.; Szwarc, M. *Polymer* **1964**, *5*, 54; *J. Phys. Chem.* **1965**, *69*, 612.
(2) Figini, R. V. *J. Polym. Sci., Part C* **1967**, *16*, 2049.
(3) Misra, N.; Mandel, M. *Macromolecules* **1984**, *17*, 495.
(4) Hara, M.; Eisenberg, A.; Storey, R. F.; Kennedy, J. P. In *Coulombic Interactions in Macromolecular Systems*; ACS Symposium Series 302; American Chemical Society: Washington, DC, 1986; p 176.
(5) Morawetz, H.; Wang, Y. *Macromolecules* **1988**, *21*, 107.
(6) Morawetz, H. *J. Lumin.* **1989**, *59*, 43.
(7) Makowski, H. S.; Lundberg, R. D.; Westerman, L.; Bock, J. *Polym. Prepr., Am. Chem. Soc. Div. Polym. Chem.* **1978**, *19*, 292.
(8) Thomas, J. K.; Dowling, K. C. *Macromolecules*, preceding paper in this issue.
(9) Roche, E. J.; Stein, R. S.; MacKnight, W. J. *J. Polym. Sci., Polym. Phys. Ed.* **1980**, *18*, 1035.
(10) Debeye, P. *Trans. Electrochem. Soc.* **1942**, *82*, 205.
(11) Noyes, R. M. *Prog. React. Kinet.* **1961**, *1*, 131.
(12) Fredrickson, G. H.; Frank, C. W. *Macromolecules* **1983**, *16*, 572.
(13) Itagaki, H.; Horrie, K.; Mita, I. *Macromolecules* **1983**, *16*, 1395.
(14) Eisenberg, A. *Macromolecules* **1970**, *3*, 147.
(15) Neppel, A.; Butler, I. S.; Brockman, N.; Eisenberg, A. *J. Macromol. Sci.* **1981**, *B19*, 61.
(16) Lantman, C. W.; MacKnight, W. J.; Higgins, J. S.; Peiffer, D. G.; Sinha, S. K.; Lundberg, R. D. In *Multiphase Polymers: Blends and Ionomers*; Utracki, L. A., Weiss, R. A., Eds.; ACS Syposium Series 395; American Chemical Society: Washington, DC, 1989; p 459.
(17) Pedley, A. M.; Higgins, J. S.; Peiffer, D. G.; Burchard, W. *Macromolecules* **1990**, *23*, 1434.
(18) Lundberg, R. D.; Makowski, H. S. *J. Polym. Sci., Polym. Phys. Ed.* **1980**, *18*, 1821.
(19) Lundberg, R. D.; Phillips, R. R. *J. Polym. Sci., Polym. Phys. Ed.* **1982**, *20*, 1143.
(20) Erdi, N. Z.; Morawetz, H. *J. Colloid Sci.* **1964**, *19*, 708.